

INSTITUTE OF PLASMA PHYSICS

NAGOYA UNIVERSITY

RESEARCH REPORT

NAGOYA, JAPAN

Electrostatic Low-Frequency Instability
of Cylindrical Tokamak

Sanae Inoue, Kimitaka Itoh
and
Shoichi Yoshikawa[†]

IPPJ - 340

June 1978

Further communication about this report is to be sent to the Research Information Center, Institute of Plasma Physics, Nagoya University, Nagoya, Japan.

Permanent Address :

Department of Physics, Faculty of Science, University of Tokyo,
Tokyo 113, Japan.

[†] Plasma Physics Laboratory, Princeton University, Princeton,
N.J. 08540, U.S.A.

Abstract

We present a comprehensive theory of the electrostatic low frequency instabilities of a collisionless plasma in a cylindrical tokamak. The plasma carries a longitudinal current which produces the poloidal magnetic field and the magnetic shear. The effects of inhomogeneities (density, electron and ion temperature gradients), plasma current, radial electric field and the magnetic shear are examined. The instabilities are found to be excited owing to the plasma current, ion temperature gradient and radial electric field, though the magnetic shear has a prominent stabilization power. The off-resonant instability in the absence of the magnetic shear is also discussed.

§I Introduction

Drift instabilities have been subject to extensive investigations concerning to the anomalous loss of magnetically confined plasmas.^{1,2)} Driving mechanisms of drift instabilities which grow by extracting energy from the mean plasma flow via electrons have been found in various parameter regimes³⁻⁵⁾.

To understand the anomalous transport processes in confined plasmas, we have to take hold of the behavior of these instabilities in a considered configuration, totally and continuously in parameter spaces. Then we are able to plan devices and search for optimum condition in experiments.

It is one of our purposes of this paper to understand kinds of electro-static (E·S) drift wave fluctuation in a sheared magnetic field. Among various kinds of drift modes, some are completely stabilized by the strong shear and the other are a little stabilized because of their nature of the mode structure (eigen value and eigen function etc.); i.e., the manner of relieving the shear effect is different. In addition, in tokamaks the magnetic shear is generated by the toroidal current which becomes the source of the current driven mode. Therefore it is important to arrange the complex situation consistently in the parameter regimes.

In a magnetic field with shear, the parallel wave number ($\vec{k} \cdot \vec{B} / B$) becomes a function of the distance in the direction of the density gradient \hat{x} . As a result, the magnetic shear results in an "effective potential" in the differential equation that governs the x-profile of perturbations

Rukhadze and Silin have tabulated many kinds of drift wave instabilities and the critical shear parameters for stability³⁾. However, the method of geometrical optics they have used is not proper to this problem because of the rapid spatial change of the "potential" in the differential equation. Employing Weber type solutions, Pearlstein and Berk (PB) have formulated and solved the differential equation,⁶⁾ demonstrating the existence of physically meaningful eigen function. However they have treated the deviation of the electron response from the Boltzmann distribution as a perturbation, and have evaluated it without consistent ordering. Taking the full non-Boltzmann part of the electron response into account, recent theoretical development on the universal mode has clarified that the universal mode is stabilized with a weak magnetic shear in a slab geometry.^{7,8)} In the previous work⁹⁾, we have made clear the discrepancy between these works and the PB theory by employing a self-consistent ordering in evaluation of the non-Boltzmann part of the electron response which determines the growth rate. It has also been shown that the current-driven (CD) drift mode becomes unstable when the magnetic shear is fairly weak.⁹⁾

In this article we investigate the drift wave instabilities of the plasma column in a helical magnetic field. According to the finite size of plasma radius, we have three typical cases of the shear parameter; $\Delta(k_{\parallel}/\omega) > 1/v_i$, $1/v_i \gg \Delta(k_{\parallel}/\omega) \gg 1/v_e$ and $1/v_e \gg \Delta(k_{\parallel}/\omega)$, where $\Delta(A)$ shows $(A_{\max} - A_{\min})$ over the plasma column. In the first case, which is for the ordinary tokamak discharge, the mode structures are approximated by those in a slab case.

In the second case, the radial drift mode structure is not out-going type, and in the last case we have the off-resonant instability which is driven by inhomogeneities. The 1st case is mainly discussed in this article. Employing orthonormal function series,⁹⁾ we rewrite the differential equation into a matrix formulation. Then we introduce a smallness parameter to truncate this matrix to find the eigen mode structure. We examine the stabilizing efficiency of the magnetic shear to various drift modes in order to seek the dominant instability out from the complex situation where driving mechanisms of instabilities are co-existing. This investigation allows us to know the optimum condition in parameter spaces for plasma confinement. For instance, the optimum plasma density may be determined through the competition between the current-driven universal mode and the collisional mode.¹⁰⁾

The structure of this paper is as follows. In §2 we discuss the Vlasov equilibrium of cylindrical plasma by use of the tokamak ordering. In §3 we derive the differential eigen-equation, and present the method of orthonormal function series in §4. We apply this principle to various kinds of modes and obtain the growth rate, the eigen function and the threshold shear for stability. In the Appendix we briefly discuss the case where magnetic shear is extremely weak.

§ 2 Equilibrium Theory

In this section, we derive the self-consistent Vlasov equilibrium of an inhomogeneous current-carrying plasma column. The equilibrium magnetic configuration is illustrated in Fig.1. A plasma column is immersed in a strong longitudinal magnetic field B_{z0} and the longitudinal current produces the poloidal magnetic field. The poloidal and longitudinal components form the helical magnetic field with a shear. We introduce the cylindrical coordinates (r, θ, z) with the z axis coinciding the magnetic axis. We assume that 1) the equilibrium has longitudinal and cylindrical symmetry ($\partial/\partial z = \partial/\partial \theta = 0$), 2) the azimuthal symmetry of the tokamaks is replaced by the longitudinal periodicity $2\pi R$, 3) the plasma temperature is high enough that the plasma is considered to be collisionless, 4) the longitudinal current is carried by electrons, 5) the plasma is low β , i.e., $\beta < M_e/M_i$ (electron to ion mass ratio), and 6) the ion gyroradius is much smaller than the scale length of inhomogeneties.

The conservation quantities of a plasma particle are the total energy H , and the two components of canonical momentum P_θ and P_z ,

$$H = \frac{1}{2} M_j v^2 + e_j \Psi(r), \quad (1)$$

$$P_\theta = r \left[M_j v_\theta + \frac{1}{c} e_j A_\theta(r) \right], \quad (2)$$

$$P_z = M_j v_z + \frac{1}{c} e_j A_z(r) , \quad (3)$$

where $\Psi(r)$ is the static potential, j denotes the species of particles and \vec{A} is the vector potential. Because the plasma is low β , $A_\theta(r)$ can be approximately given by

$$A_\theta(r) = \frac{1}{2} B_{z0} r \quad (4)$$

with the aid of the tokamak ordering, $(B_\theta/B_{z0})^2 = r^2/q^2 R^2 \ll 1$, where $B_{z0} = B_z(r=0)$. Thus

$$P_\theta = \frac{1}{2c} B_{z0} e_j \left(r^2 + \frac{2r v_\theta}{\Omega_j} \right) \quad (2')$$

with $\Omega_j = e_j B_{z0}/M_j c$ is the cyclotron frequency. Using two constants of motion, Eqs. (2) and (3), we have the other constant of motion

$$P_{||} = M_j \left(v_z + \frac{B_\theta}{B_{z0}} v_\theta \right) . \quad (3')$$

We also have the constant of motion

$$H - e_j \Psi(\sqrt{2r v_\theta/\Omega_j + r^2}) \approx \frac{1}{2} M_j v^2 + \frac{1}{\Omega_j} e_j E_r v_\theta \quad (1')$$

expanding Ψ with respect to $r v_\theta/\Omega_j$.

An equilibrium distribution function f_0 is given in terms of constants of motion. The three constants of motion, Eqs. (1') (2') and (3') are used to form the distribution having the desired density, temperature and velocity inhomogeneities as

$$f_0 = \frac{n_0}{(2\pi v_{T0}^2)^{3/2}} \exp \left\{ -\frac{(r^2 + 2r v_\theta/\Omega_j)}{2L_n^2} - \frac{(r^2 + 2r v_\theta/\Omega_j)(v^2 + 2eME_r v_\theta/\Omega_j)}{L_T^2 2v_{T0}^2} \right\}$$

$$- \frac{v^2 + 2eM\bar{E}rV_{\theta}/\Omega - 2u(v_z + v_{\theta} B_{\theta}/B_{z0}) + u^2}{2v_{T0}^2} \left\{ \left[1 + \frac{(r^2 + 2rV_{\theta}/\Omega)}{L_T^2} \right]^{\frac{3}{2}} \right.$$

with

(5)

$$u = u_0 \left\{ 1 - \left(r^2 + \frac{2rV_{\theta}}{\Omega} \right) / L_u^2 \right\},$$

where the notation j is suppressed. The quantities n_0 , u_0 and v_{T0} are the particle density, the flow velocity and the thermal speed at $r = 0$. We take $u = 0$ for ions. The fundamental three moments are

$$n = n(r) = n_0 \exp\left(-\frac{r^2}{2L_n^2}\right), \quad (6)$$

$$\vec{V} = \vec{V}(r) = -\frac{v_T^2}{\Omega} \left\{ \frac{r}{L_n^2} + \frac{2r}{(L_T^2 + r^2)} \right\} \hat{\theta}.$$

$$- \frac{c}{B_{z0}} E_r \hat{\theta} \quad (7)$$

$$+ u_0 \frac{(1 - r^2/L_u^2)}{(1 + r^2/L_T^2)} \left\{ \hat{z} + \frac{B_{\theta}}{B_{z0}} \hat{\theta} \right\},$$

and

$$T = T(r) = \frac{T_0}{1 + r^2/L_T^2}. \quad (8)$$

Here we have assumed $(\rho_i/L_n)^2$, $(B_{\theta}/B_z)^2$, and $(ru/v_e L_u)^2 \ll 1$ with $\rho_i = v_i/\Omega_i$ and $v_j^2 = T_j(r)/M_j$. The terms in the right hand side of Eq. (7) stand for the diamagnetic flow, $\vec{E} \times \vec{B}$ flow and the force free current. Eqs. (6)-(8) satisfy the equilibrium equation

$$\vec{j} \times \vec{B} = \nabla p . \quad (9)$$

The poloidal magnetic field is derived from the force free current through the maxwell's equation $\nabla \times \vec{B} = 4\pi\vec{j}/c$ as

$$B_{\theta} = -\frac{4\pi e}{cr} \int_0^r n v_z r dr . \quad (10)$$

Thus the equation (5) is the self-consistent Vlasov equilibrium solution of the inhomogeneous current-carrying plasma column in the limit of the tokamak ordering and low β approximation. Figure 2 illustrates the typical example of the radial distribution of j_z , B_{θ} and $q(r)$ (q : the safety factor $B_{z0}r/B_{\theta}R$).

For the cylindrical plasma column the shear length L_s is defined by

$$\frac{1}{L_s} = \left| \frac{1}{k} \frac{d}{dr} \left(\frac{\vec{k} \cdot \vec{B}}{B} \right) \right| , \quad (11)$$

where $\vec{k} = (0, m/r, n/R)$, ($m, n = 1, 2, 3 \dots$) and $1/L_s$ is evaluated by

$$\frac{1}{L_s} = \left| \frac{r}{R} \frac{d}{dr} \left(\frac{B_{\theta}R}{B_{z0}r} \right) \right| .$$

The density gradient scale, $\kappa \equiv -\nabla n/n$ is given by $+r/L_n^2$.

The temperature gradient scale is written $\kappa_T = -\nabla T/T$.

We also use the notation $\eta_j \equiv \kappa_{Tj}/\kappa_j$.

§ 3 Linearized Theory

Since we consider the low β plasma, we introduce an electrostatic potential perturbation $\phi(\vec{x}, t)$. From the periodicity we consider a Fourier component $\phi(\vec{x}, t) = \phi_{m\ell}(r) e^{i(m\theta + \ell z/R - \omega t)}$. The mode is labeled by poloidal and longitudinal mode numbers m and ℓ . On the other hand, the potential perturbation is localized in the neighbourhood of the mode-rational surface r_s where $q(r_s) = m/\ell$ holds. Thus, in the following analysis we discriminate the mode by m and r_s and suppress the suffixes m and r_s .

We take the linearized Vlasov equation. The perturbed distribution function $\tilde{f}(\vec{x}, \vec{v}, t)$ can be written in terms of the characteristic integral as

$$\tilde{f}(\vec{x}, \vec{v}, t) = \frac{e_j}{M_j} \int_{-\infty}^t dt' \nabla' \Phi(\vec{x}', t') \cdot \nabla_{\vec{v}'} f_0(\vec{x}', \vec{v}') \quad (12)$$

where (\vec{x}', \vec{v}', t') is the particle trajectory variables and ∇' and $\nabla_{\vec{v}'}$ are the derivative with respect to \vec{x}' and \vec{v}' respectively. Using the constants of motion and the relation $d\Phi(\vec{x}', t')/dt' = \partial\Phi/\partial t' + \vec{v}' \cdot \nabla' \Phi$, we find the Fourier coefficient of \tilde{f} , $\tilde{f} \equiv \bar{f}(r, \vec{v}) e^{i(m\theta + \ell z/R - \omega t)}$ as

$$\begin{aligned} \bar{f}(r, \vec{v}) = & -f_0 \frac{e}{T_0} \left[\left\{ 1 + (r^2 + \frac{2rV_\theta}{\Omega}) / L_T^2 \right\} \phi(r) \right. \\ & \left. + i \left\{ \left(1 + \frac{r^2 + 2rV_\theta/\Omega}{L_T^2} \right) \omega - m \left(1 + \frac{r^2}{L_T^2} \right) \left\{ \omega_{dj} + \omega_{Tj} \left(\frac{v^2}{v_{T0}^2} - \frac{3v_T^2}{v_{T0}^2} \right) - \frac{2u_0(v_z - u)}{\Omega L_n^2} \right\} \right] \end{aligned}$$

$$-m \left(1 + \frac{r^2 + 4r\bar{v}_\theta / R_0}{L_T^2} \right) \omega_E - k_{\parallel} u \left. \right\} I(r) \quad (13)$$

where $\omega_{dj} = -cT_j / eB_{z0} L_n^2$, $\omega_{Tj} = L_n^2 \omega_d / L_T^2$, $k_{\parallel} = \vec{k} \cdot \vec{B} / B_{z0}$, $\omega_{Ej} = -cm(E_r + \rho_j^2 E_r'' / 2) / rB_{z0}$ and

$$I(r) = \int_{-\infty}^{\infty} d\tau \phi(r') \exp[-i\omega\tau + im(\theta' - \theta) + il(z' - z)/R] \quad (14)$$

In order to evaluate $I(r)$, we introduce new variables of the particle velocity (v_{\perp} , v_{\parallel} , p) to obtain the particle trajectory with the help of the tokamak ordering

$$r' - r = \frac{v_{\perp}}{\Omega} [\sin(\Omega\tau - p) + \sin p] ,$$

$$r(\theta' - \theta) = \frac{v_{\perp}}{\Omega} [\cos(\Omega\tau - p) - \cos p] - \frac{cE_r}{B_{z0}} + \frac{B_{\theta}}{B_{z0}} v_{\parallel} \tau , \quad (15)$$

$$z' - z = v_{\parallel} \tau ,$$

where we have assumed that the equilibrium quantity varies much slower than the ion gyroradius. We also assume that the radial variation of the potential fluctuation ϕ is slow compared with the particle gyroradius. We expand ϕ into a Taylor series around the rational surface, and retain terms up to the 2nd order in $\rho^2 \frac{d^2}{dr^2}$ as

$$\phi(r') = \phi(r) + (r' - r) \phi'(r) + \frac{1}{2} (r' - r)^2 \phi''(r) + \dots \quad (16)$$

Substituting Eqs. (15) and (16) into Eq. (14), we obtain in the low frequency limit ($|\omega - k_{\parallel} v_{\parallel} - m\omega_E| \ll \omega_c$)

$$I(r) = i \frac{\exp[-i(\frac{mV_{\perp}}{\Omega r}) \cos p]}{\omega - m\omega_E - k_{\parallel} v_{\parallel}} \left[J_0\left(\frac{mV_{\perp}}{\Omega r}\right) \left(\phi + \frac{V_{\perp}}{\Omega} \sin p \frac{d\phi}{dr} \right) + \left(\frac{V_{\perp}}{\Omega r}\right)^2 \left\{ (1+2\sin^2 p) J_0\left(\frac{mV_{\perp}}{\Omega r}\right) + J_2\left(\frac{mV_{\perp}}{\Omega r}\right) \right\} \frac{d^2\phi}{dr^2} \right] \quad (17)$$

where $m\omega_E = -ce_r m/rB_{z0}$ is the doppler shift due to the $\vec{E} \times \vec{B}$ drift. Performing the integration of \bar{f} over $d^3v = dp dv_{\parallel} v_{\perp} dv_{\perp}$ we get the density perturbations of electrons and ions as,

$$\frac{\bar{n}_e}{n_e} = \frac{e\phi}{T_e} \left[1 + \frac{\omega - m\omega_{de} + \frac{m}{2}\omega_{Te} - m\omega_E - k_{\parallel} u}{\omega - m\omega_E - k_{\parallel} u} \xi_e Z(\xi_e) - \frac{m\omega_{Te}}{\omega - m\omega_E - k_{\parallel} u} \xi_e^2 \left\{ 1 + \xi_e Z(\xi_e) \right\} - \frac{m u_0}{\Omega L_u^2 k_{\parallel}} \left\{ 1 + \xi_e Z(\xi_e) \right\} - \frac{m u u_0}{\Omega L_u^2 (\omega - m\omega_E - k_{\parallel} u)} \xi_e Z(\xi_e) \right] \quad (18)$$

and

$$\frac{\bar{n}_i}{n_i} = -\frac{e\phi}{T_e} \left[\frac{\omega + m\omega_{di} - \frac{m}{2}\omega_{Ti} - m\omega_E}{\omega - m\omega_E} + \frac{m\omega_{Ti}}{\omega - m\omega_E} \xi_i^2 \left\{ 1 + \xi_i Z(\xi_i) \right\} + \frac{m\omega_{Ti}}{\omega - m\omega_E} \xi_i Z(\xi_i) \frac{(b\Lambda)'}{\Lambda'} \right] \frac{-b\Lambda'}{k^2} \frac{d^2\phi}{dr^2}$$

$$\begin{aligned}
& + \left[1 + \frac{\omega + m\omega_{di} - \frac{m}{2}\omega_{Ti}}{\omega - m\omega_E} \xi_i Z(\xi_i) \Lambda + \frac{m\omega_{Ti}}{\omega} \xi_i^2 \{1 + \xi_i Z(\xi_i)\} \Lambda \right. \\
& \left. + \frac{m\omega_{Ti}}{\omega} \xi_i Z(\xi_i) b \Lambda' \right] \phi(r) \quad (19)
\end{aligned}$$

where $\xi_e \equiv (\omega_{//} - k_{//}u - m\omega_E)/\sqrt{2}|k_{//}|v_e$, $\xi_i \equiv (\omega - m\omega_E)/\sqrt{2}|k_{//}|v_i$, $b \equiv (mv_{Ti}/r\Omega_i)^2$, $\Lambda(b) = I_0(b)e^{-b}$, $\Lambda' = \partial\Lambda/\partial b$, $I_0(b)$ is the 0th order modified Bessel function, and Z is the plasma dispersion function defined by

$$Z(\xi) = \frac{1}{\sqrt{\pi}} \int_{-\infty}^{\infty} dt \frac{e^{-t^2}}{t - \xi}.$$

For a plasma composed of electrons and singly charged ions, the Poisson equation gives the differential dispersion equation. Neglecting $k^2\lambda_D^2$ compared to unity (λ_D : Debye length) we have

$$\begin{aligned}
& -\Lambda' \tau \left[\frac{\tilde{\omega} + m\omega_{di} - \frac{m}{2}\omega_{Ti}}{\tilde{\omega}} \xi_i Z + \frac{m\omega_{Ti}}{\tilde{\omega}} \xi_i^2 \{1 + \xi_i Z(\xi_i)\} + \frac{m\omega_{Ti}}{\tilde{\omega}} \xi_i Z(\xi_i) \frac{(b\Lambda)'}{\Lambda'} \right] \\
& \quad \times \rho_i^2 \frac{d^2\phi}{dr^2} \\
& + \left[1 + \frac{\tilde{\omega} - m\omega_{de} + \frac{m}{2}\omega_{Te} - k_{//}u}{\tilde{\omega} - k_{//}u} \xi_e Z(\xi_e) - \frac{m\omega_{Te}}{\tilde{\omega} - k_{//}u} \xi_e^2 \{1 + \xi_e Z(\xi_e)\} \right. \\
& \quad \left. - \frac{m u_0}{\Omega L_u^2 k_{//}} \{1 + \xi_e Z(\xi_e)\} - \frac{m u_0}{\Omega L_u^2 (\tilde{\omega} - k_{//}u)} \xi_e Z(\xi_e) \right]
\end{aligned}$$

$$\tau \left\{ 1 + \frac{\tilde{\omega} + m\omega_{ci} - \frac{m}{2}\omega_{Ti}}{\tilde{\omega}} \xi_i Z(\xi_i) \Lambda + \frac{m\omega_{Ti}}{\omega} \xi_i^2 \left\{ 1 + \xi_i Z(\xi_i) \right\} \Lambda \right. \\ \left. + \frac{m\omega_{Ti}}{\omega} \xi_i Z(\xi_i) b \Lambda' \right\} \phi = 0 \quad (20)$$

where $\tau = T_e/T_i$, $\tilde{\omega} = \omega - m\omega_E$. The terms proportional to u_0/L_u^2 are due to the velocity shear of electrons. Since the wave is localized in the vicinity of the rational surface where $\vec{k} \cdot \vec{B} = 0$ ($r = r_s$), we expand k_{\parallel} as $k_{\parallel} = 2m r_s (r - r_s) / qRL_p^2$, and solve Eq. (20) in the drift limit $\omega \gg |k_{\parallel}| v_i$. We expand $Z(\xi_i)$ in Eq. (20) with respect to $1/\xi_i$ and obtain the basic equation in dimensionless form as

$$\frac{d^2\phi}{d\zeta^2} + \left[\lambda + \tilde{\mu}^2 \zeta^2 + \sigma(\zeta) \right] \phi = 0 \quad (21)$$

where

$$\zeta = (r - r_s) / \tilde{\rho}_i^2, \quad \tilde{\rho}_i^2 = -\Lambda' \rho_i^2, \quad \tilde{\zeta} = (\tau\omega + \omega_*) \Lambda + \omega_{*T} b \Lambda'$$

$$\lambda = \frac{\Lambda' \tilde{\zeta} - (1 + \tau) \omega \Lambda'}{(\tau\omega + \omega_*) \Lambda' + \omega_{*T} (b \Lambda')}, \quad \mu^2 = \frac{\Lambda' (\tilde{\zeta} + \omega_{*T} \Lambda)}{\tilde{\zeta}'}, \quad \frac{k^2 v_i^2 \tilde{\rho}_i^2}{L_s^2 \tilde{\omega}^2},$$

$$\tilde{\mu}^2 = \mu^2 + \frac{\Lambda'}{\tilde{\zeta}'} \left[\tau\omega \Lambda' + \left(1 + \frac{\tau\omega \Lambda'}{\tilde{\zeta}'} \right) \left\{ (1 + \tau)\omega - \tilde{\zeta} \right\} \right] \frac{m\omega_E}{\tilde{\omega}},$$

$$\omega_{Ei} = \omega_{Ei0} + \omega_{E2} \frac{(r - r_s)^2}{\tilde{\rho}_i^2}, \quad \tilde{\omega} = \omega - \omega_{Ei0}, \quad \tilde{\omega}_e = \omega - \omega_{Ee'}$$

and

$$\sigma = -\frac{\tilde{\omega} \Lambda'}{\tilde{\zeta}'} \left[\frac{\tilde{\omega}_e - m \omega_{de} + \frac{m}{2} \omega_{Te} - k_{\parallel} u}{\tilde{\omega} - k_{\parallel} u} \sum_{\xi_e} Z(\xi_e) \right. \\ \left. - \frac{m \omega_{Te}}{\tilde{\omega}_e - k_{\parallel} u} \xi_e^2 \{1 + \xi_e Z(\xi_e)\} - \frac{m u_0}{\Omega L_u^2 k_{\parallel}} \left\{ 1 + \frac{\tilde{\omega}_e}{\tilde{\omega}_e - k_{\parallel} u} \xi_e Z(\xi_e) \right\} \right]$$

where $\omega_* = \tau m \omega_{di}$ and $\omega_{*T} = \tau m \omega_{Ti}$. We also introduce the parameter ζ_e as $\tilde{\omega}/k_{\parallel} v_e = \zeta_e/\zeta$. The electron velocity shear terms in σ are dropped in the following analysis because $u_0 \rho_e / v_e L_u \ll 1$ holds. When the wave localization width δ is smaller than r_s , the coefficients λ , $\tilde{\mu}^2$ and σ are evaluated by the value at $r = r_s$. The basic equation is very similar to the one obtained in the slab geometry as is expected. We discuss in the Appendix the case that δ is order of the several times of the plasma radius a . Note that μ^2 can become negative when the ion temperature gradient is large enough.

§ 4 Stability Analysis

To determine the stability properties of the current-driven universal drift mode of the cylindrical plasma column, we rewrite the differential equation (21) into a matrix equation as the case of a slab model. In the following, the r dependence of b , λ and μ is neglected in Eq. (21).

In the first place we obtain the real frequency of the mode. Neglecting the electron resonance term in Eq. (21) we have

$$\left[\frac{d^2}{d\zeta^2} + \lambda + \tilde{\mu}^2 \zeta^2 \right] \phi = 0. \quad (22)$$

We use the orthonormal set $\{\phi_n(\zeta) | \phi_n(\zeta) = \sqrt{\frac{i\tilde{\mu}}{\pi}} \sqrt{\frac{1}{n!}} H_n(\sqrt{2i\tilde{\mu}} \zeta) e^{-i\tilde{\mu}\zeta^2/2}\}$ on which the boundary conditions that the wave is out-going and ϕ is regular at $\zeta = 0$ are imposed.⁹⁾

Each ϕ_n satisfies

$$\left[\frac{d^2}{d\zeta^2} + \lambda_n + \tilde{\mu}^2 \zeta^2 \right] \phi_n = 0, \quad \lambda_n = i\tilde{\mu}(2n+1). \quad (23)$$

Thus the eigen value is given as

$$\lambda = \lambda_n, \quad (24)$$

showing that each ϕ_n is the eigen function of the mode when the electron response is the Boltzmann distribution, $\sigma=0$. Writing $\omega = \omega_0 + i\gamma$ and linearizing λ with respect to γ/ω_* , ω_0 and γ are given as $\lambda(\omega = \omega_0) = 0$ and $\gamma = -\mathfrak{E} \text{Im}\lambda/\Lambda'(1+\tau-\tau\Lambda)$. The real frequency is given by

$$\omega_0 = \frac{\Lambda + b\Lambda'\eta_i}{1 + \tau - \tau\Lambda} \omega_* \quad (25)$$

and the imaginary part is found from Eq. (24) to be

$$\gamma = -(2n+1) \tilde{\mu} \frac{E'}{\Lambda'(1+\tau-\tau\Lambda)} \quad (26)$$

which represents the convective damping due to the magnetic shear. The competition between the convective damping and the excitation by the electron resonance determines the stability as will be shown below.

It should be noted again that $\tilde{\mu}^2$ can become negative. When $\tilde{\mu}^2 < 0$ holds, the eigen modes become localized type as $\phi_n \propto e^{-|\tilde{\mu}|\zeta^2/2}$ and all λ_n become real, so that the convective damping is annihilated. Figure 3 shows the regions where $\mu^2 < 0$ holds or $\omega < 0$ holds in the case $E_r = 0$. When κ_{T_i}/κ is large enough, $\mu^2 < 0$ holds and the convective damping vanishes.

As easily known from Eq. (21), the uniform rotation part of ω_E, ω_{E0} , only causes the real frequency shift and has no substantial effect on the stability. On the other hand, the curvature of the static electric field E_r affects the stability. When E_r has the negative curvature, i.e. $E_r'' < 0$, the convective damping of the wave increases, and when $E_r'' > 0$, the convective damping is reduced.

In the presence of the electron resonance, ϕ_n 's couple and the normal mode $\phi(\zeta)$ can be expressed as

$$\phi(\zeta) = \sum_{n=0}^{\infty} a_n \phi_n(\zeta). \quad (27)$$

We first give a general note on the mode structure $\phi(\zeta)$. The inhomogeneity driven part of the electron resonance, $\xi_e \exp(-\xi_e^2) \times (\omega_* - \omega - \omega_* \eta_e / 2)$, couples ϕ_{2n} mode and the even mode is decoupled from the odd mode. On the other hand, the current driven part couples ϕ_{2m+1} with ϕ_0 , which is the least stable mode in the absence of the electron resonance. Thus we cannot neglect the mixing of the even and the odd modes.

Substituting Eq. (27) into Eq. (21), we have

$$0 = \begin{pmatrix} \lambda - \lambda_0 + V_{00} & , & V_{01} & , & V_{02} & , \dots \\ V_{10} & , & \lambda - \lambda_1 + V_{11} & , & V_{12} & , \dots \\ V_{20} & , & V_{21} & , & \lambda - \lambda_2 + V_{22} & , \dots \\ \dots & & \dots & & \dots & \dots \end{pmatrix} \begin{pmatrix} a_0 \\ a_1 \\ a_2 \\ \dots \end{pmatrix}, \quad (28)$$

where

$$V_{ij} = \langle i | \sigma | j \rangle \equiv \int_{-\infty}^{\infty} \phi_i(\zeta) \sigma(\zeta) \phi_j(\zeta) d\zeta,$$

and $\langle i|j \rangle = \delta_{ij}$ is the Kronecker delta. The eigen value equation is given by

$$\det \begin{vmatrix} \lambda - \lambda_0 + V_{00} & V_{01} & \dots \\ V_{10} & \lambda - \lambda_1 + V_{11} & \dots \\ \dots & \dots & \dots \end{vmatrix} = 0. \quad (29)$$

In the case of the nonelectron-resonance limit, we of course have $\lambda = \lambda_n$ with $\{a_{in}\} = \{\delta_{m,n}\}$. One way of handling Eq. (29) is the truncation of the matrix, which gives the hierarchy of approximation. Another way is the expansion with respect to some smallness parameter, if any. In case where the coupling with high n modes are crucial to the stability, the latter method is appropriate. We are interested in the strong shear case

$$1 < \frac{\gamma_s L_s}{L_n^2} \ll \frac{M_i}{M_e} \quad (30)$$

and we take

$$\epsilon \equiv \sqrt{|\mu|} \zeta_e \sim O(\sqrt{\kappa L_s M_e / M_i})$$

as a smallness parameter and retain up to the order of $\epsilon \ln \epsilon$. Taking all effects by the even components ϕ_{2n+2} and odd components ϕ_{2n+1} ($n = 0, 1, 2, \dots$) on the least stable

components ϕ_0 , we have an approximate solution of Eq. (29) as

$$1 + \sum_{n=0}^{\infty} \frac{V_{2n,2n}}{\{\lambda - (4n+1)i\mu\}} - \sum_{n=0}^{\infty} \frac{V_{2n+1,0}^2}{\{\lambda - (4n+3)i\mu\} \{\lambda - i\mu\}} = 0, \quad (32)$$

where

$$V_{2n,2n} = \frac{(2n-1)!!}{(2n)!!} (i-1) \frac{\Lambda'(\omega_* - \omega - \eta_e \omega_*/2)}{\Sigma'} \epsilon \ln \frac{\sqrt{2}}{\epsilon}, \quad (33)$$

$$V_{2n+1,0} = \frac{(2n-1)!!}{\sqrt{(2n+1)!}} (-1)^n i \frac{\Lambda' \omega u}{\Sigma' v_e}, \quad (34)$$

in the lowest order of ϵ . The equation (32) shows the competition between the electron resonance and the shear convective damping. Equations (32), (33) and (34) are rewritten as

$$1 - \frac{(1+i)}{4\mu} \frac{\Lambda'(\omega_* - \omega - \omega_* \eta_e/2)}{\Sigma'} \frac{\sqrt{\pi} \Gamma(\frac{1}{4} + \frac{i\lambda}{4\mu})}{\Gamma(\frac{3}{4} + \frac{i\lambda}{4\mu})} \epsilon \ln \frac{\sqrt{2}}{\epsilon} + \frac{\pi}{2} \frac{1}{(\lambda - i\mu)^2} \left[\frac{\Lambda' \omega u}{\Sigma' v_e} \right]^2 \left[1 - \frac{\Gamma(\frac{3}{4} + \frac{i\lambda}{4\mu})}{\sqrt{\pi} \Gamma(\frac{5}{4} + \frac{i\lambda}{4\mu})} \right] = 0, \quad (35)$$

which is the dispersion relation to determine the eigen value λ . The normal mode is

$$\phi = \phi_0 - \sum \frac{V_{2n,0} \phi_{2n}}{\lambda - (4n+1)i\mu} - \sum \frac{V_{2n+1,0} \phi_{2n+1}}{\lambda - (4n+3)i\mu}. \quad (36)$$

As easily known, the even mode and the odd mode decouples when $u/v_e = 0$. In the case of $u/v_e = \eta_e = \eta_i = 0$, Eq. (35)

is equivalent , in the lowest order of ϵ , to the dispersion relation obtained in Eq. (25) of the ref. [11]. In addition to it, Eq. (35) enables us to consider the combined effect of the inhomogeneities, static electric field, and the plasma current on the stability.

The equation (35) shows instability when the plasma current is large enough. If we limit ourselves to the case where $\eta_i = \eta_e = 0$ and $\omega = \omega_*$, Eq. (35) gives the critical shear condition for stability

$$\frac{1}{\kappa L_S} > 0.61 \frac{\tau}{1 + \tau} \frac{u}{v_e} \quad (37)$$

which agrees with the result in Ref. [12] apart from a numerical factor of order of unity. We solve Eq. (35) for typical cases and show the growth rate in Eqs.4-7. The Figure 4 illustrates γ (normalized to ω_*) as a function of b for the parameters $\kappa L_S = 8, 16$ and 32 ($\kappa_{Te} = \kappa_{Ti} = u/v_e = 0$). It is shown that the universal mode is marginally stable when b exceeds the critical value. The electron temperature gradient is not enough to excite the drift wave even if $\kappa_{Te}/\kappa < 0$ holds (Fig.5), while the electron current can excite the drift wave as illustrated in Fig.6. In the presence of the electron current, the concept of the critical shear is still important. Fairly long wave length modes have large growth rate. In Fig. 7 the growth rate is shown, in the presence of electron temperature gradient and electron current, as a function of b for the shear parameters $\kappa L_S = 12, 20, 32$ and 50 . It is shown that the electron temperature gradient tends to stabilize the mode

but not enough to completely suppress the instability when the magnetic shear is below the critical value for stability.

We understand the fact that universal mode is stable as follows. When the magnetic shear is present, the source term $\sigma(\zeta)$ is localized near the rational surface; this spatial variation of σ causes the coupling of the principal ($n = 0$) mode with higher $2n$ modes. Such high n modes carry the free energy away from the interaction region (since $\lambda_n \propto 2n + 1$). The convective damping of the mode is effectively enhanced. Thus, we note the magnetic shear has three effects on drift instabilities; convective damping, localization of σ (which naturally reduces growth rate) and the coupling of the principal mode with high $2n$ modes. The stability is determined by the balance between the convective damping, high $2n$ coupling and the inhomogeneity driving source. For the universal mode and the temperature gradient mode, $\sigma \propto 1/|\zeta|$ holds for $|\zeta| > \zeta_e$. Electron resonance term σ in one hand excites the mode, and in another hand it effectively enhances the convective damping. The result implies that the inhomogeneity driving source is insufficient to excite the instability as a whole. For the current driven mode, the instability source term $k_{\perp}u$ (= $k_{\perp}u/L_s$) is proportional to the shear strength. Thus the stability is determined not directly by the convective damping but by the localizing effect by the shear. This, we note, leads to that the instability driving term due to the current is insensitive to the shear damping and to the coupling with higher $2n + 1$ modes, which confirms the validity of the truncation of the matrix. In fact, the result is satisfactory when we keep only terms up to

V_{10}^2 ; in this approximation we recover the characteristics of the current driven drift instability except we underestimate the destabilization contribution of the plasma current.

It should be noted that the consistent ordering is the key concept to judge the stability. If one forgets the consistency in handling the electron Z function terms, one may only retain electron resonance,¹³⁾ or one may evaluate electron resonance by its value at some point⁶⁾ (for instance at turning point $\zeta = 1/\sqrt{\mu}$); these procedure merely leads to the wrong results mispredicting stability or instability.

§ 5 Discussions

In § 3, we derive the differential eigen equation for the drift waves in the sheared magnetic field, based on the equilibrium distribution function obtained in § 2. The solution is obtained by use of the orthonormal expansion method, and the effects of various inhomogeneities on the stability are examined with the shear convective damping. The section 4 is devoted to the case where a wave is well localized around the rational surface. In the low shear limit, the wave spreads over the column and the eigen value is determined by the position of edge, i.e. $m\rho_i/a$. This case is discussed in the Appendix.

When the ion temperature gradient exists, the growth rate of the current driven mode increases. The value μ becomes small as η_i increases. As μ decreases, the convective damping decreases faster than the wave localization effect does. Therefore the current destabilizing term remains large in comparison with other damping terms according to the increase of η_i . Moreover, if η_i exceeds η_0 in Fig. 3 (in regions B and D), the real frequency becomes negative and the electron temperature gradient turns to further destabilize the instability, and the ion branch may become unstable. The stability is examined for the case of $\mu^2 > 0$ in § 4. As η_i exceeds the critical value η_c , $\mu^2 < 0$ holds and the wave becomes not out-going type but localized. Thus shear convective damping is annihilated and low n ($n < \kappa L_s$) modes become unstable. (High n modes ($n > \kappa L_s$) are stabilized by the ion Landau damping.)

This implies that there is an upper bound of the ion temperature gradient experimentally (~ 1.5), and that the ion temperature gradient greater than 1.5 may not be realized.

The inhomogeneity of ω_* easily destabilizes the drift waves. When $1/L^2 = \partial^2 \omega_*/\partial r^2 / \omega_* < 0$, the wave is localized and the convective damping by the magnetic shear is reduced and even annihilated if the inhomogeneity of ω_* is strong; $L < \rho_i k L_s$. This condition is occasionally satisfied in the experiments. This explains the abundance of the excited modes which are usually observed in the experiments.^{14,15} In fact, the observed density profile in the toroidal devices are different from the gaussian distribution and ω_* is no longer a constant.

In deriving the basic equation (20), we formulate it as a 2nd order differential equation; i.e., we neglect the higher order derivatives with respect to ζ . The stability of the universal mode is found by taking the electron resonance completely. If one completely take the ion response, Eq. (20) contains higher order derivatives (or Eq. (20) turns out to be an integral equation). There remains an open question whether these higher order derivatives affect the stability or not.

By use of the mode structure obtained here, we can estimate the cross field plasma flux and derive the scaling law of plasma confinement. We discuss the electron particle and heat fluxes owing to the drift instabilities in the reference [10].

The "cylindrical tokamak" implies that we neglect the

toroidal effect of tokamaks. When the temperature becomes high enough, the trapped particles appear and the investigations derived here is incomplete to cover all parameter regimes of tokamak plasmas. We discuss the nonlocal theory of the trapped electron drift instability in another paper [16]. Of course one should not forget the electromagnetic effect on the drift wave stability for high temperature plasmas.¹⁷⁾ Thus further efforts are still required to achieve full understanding of the low frequency instabilities and the enhanced transport of tokamak plasmas.

Acknowledgements

We would like to thank Profs. T. Kamimura, K. Nishikawa and Y. Terashima for hospitalities. Numerical caluculations are performed by use of HITAC 8700/8800 Computor Center of Tokyo University and M-190 Computor Center, Institute of Plasma Physics, Nagoya University. The work has been partially supported by Scientific Research Fund of Ministry of Education, Science and Culture in Japan.

References

- 1) B. B. Kadomtsev, Plasma Turbulence (Academic Press, 1965) Chap. IV.
- 2) S. Yoshikawa and N. C. Christofilos, Plasma Physics and Controlled Nuclear Fusion Research (IAEA, Vienna 1971) 357, and the papers sited there.
- 3) A. A. Rukhadze and V. P. Silin, Soviet Physics USPEKHI 11 No.5 (1969) 659.
- 4) A. B. Mikhailovskii, Theory of Plasma Instabilities (Consultants Bureau, 1974) Vol. 2.
- 5) B. B. Kadomtsev and O. P. Pogutse, Reviews of Plasma Physics (Consultants Bureau, 1970) Vol. 5, Chap. 2.
- 6) L. D. Pearlstein and H. L. Berk, Phys. Rev. Lett. 23 (1969) 220.
- 7) D. W. Ross and S. M. Mahajan, Phys. Rev. Lett. 40 (1978) 324.
- 8) K. T. Tsang, P. J. Catto, J. C. Whitson and J. Smith, Phys. Rev. Lett. 40 (1978) 327.
- 9) S. Inoue, K. Itoh and S. Yoshikawa, Nucl. Fusion 18 No.6 (1978).
- 10) S. Inoue, K. Itoh and Y. Terashima, IPPJ-Report 318 (Nagoya 1977).
- 11) M. N. Rosenbluth and P. J. Catto, Nucl. Fusion 15 (1975) 573.
- 12) M. N. Rosenbluth and C. S. Liu, Phys. Fluids 15 (1972) 1801.
- 13) N. T. Gladd and W. Horton, Jr.) Phys. Fluids 16 (1973) 879.

- 14) S. Yoshikawa, Nucl. Fusion 13 (1973) 433 and the papers cited there.
- 15) R. J. Goldston, E. Mazzucato, R. E. Slusher and C. M. Surko, Plasma Physics and Nuclear Fusion Research (IAEA, Vienna 1976) 371.
- 16) S. Inoue, K. Itoh and S. K. Wong, GA-A14365.
- 17) S. Inoue, K. Itoh and T. Tange, IPPJ-Report 308 (Nagoya 1977).

Appendix: Extremely Weak Shear Parameter Case

When the plasma current density is flat, q-value has a weak dependence on r; thus k_{\parallel} can be considered as a constant. In this case the radial mode structure is not localized around the rational surface, but spreads over the whole column. The eigen mode structure is determined by the r-dependence of $b \equiv m^2/r^2$, ω_* This Appendix is devoted to show the typical characteristics of the drift wave in a shearless cylinder, not to give extensive parameter survey. Here we simply consider the case where r dependence is retained only for b, to show the off-resonant instability. Taking $\kappa_{Ti} = 0$ we have

$$\left[-\Lambda' \rho_i^2 \frac{\partial^2}{\partial r^2} + \Lambda(b) + C \right] \phi = 0, \quad (A1)$$

with $\Lambda(b) = I_0(b)e^{-b}$, $b = m^2/r^2$, and

$$C = \frac{(1+\tau) + \frac{(\omega - \omega_*)}{\sqrt{2}|k_{\parallel}|v_e} Z(\xi_e)}{\frac{(\tau\omega + \omega_*)}{\sqrt{2}|k_{\parallel}|v_e} Z(\xi_i)} \quad (A2)$$

Here, C is the eigen value and ω is given by Eq. (A2) once C is obtained. The boundary condition is that ϕ is regular at $r=0$ and $\phi(a)=0$. C is determined as a function of m and a/ρ_i from Eq. (A1). In Fig. A1, C is illustrated for the parameter $a/\rho_i = 100$. The n-th higher harmonics which has n nodes, has larger eigen value than the principal mode and is less dangerous. We look for an off-resonant instability. In the limit $\omega > k_{\parallel}v_e \gg k_{\parallel}v_i$, we approximately have $\xi_i Z(\xi_i) =$

- 1 and $\xi_e Z(\xi_e) = -1 - k_{\parallel}^2 v_e^2 / \omega^2$. Equation (38) can be rewritten as

$$\omega^3 + \frac{\omega_*}{\tau} \omega^2 - \frac{k_{\parallel}^2 v_e^2}{\tau(1+C)} \omega + \frac{k_{\parallel}^2 v_e^2}{\tau(1+C)} (\omega_* + \omega_T) = 0. \quad (A3)$$

ω becomes complex (which means instability) number, when

$$C < -1 + \frac{k_{\parallel}^2 v_e^2 \tau}{\omega_*^2} \frac{[9\tau(\kappa + \kappa_T) + \kappa]^2}{16\kappa[3\tau(\kappa + \kappa_T) - \kappa]}, \quad (A4)$$

is satisfied. Or writing $\omega_* = \tau \kappa k \rho_i v_i$,

$$C < -1 + \frac{k_{\parallel}^2 M_i a^2}{\kappa^2 M_e m^2 \rho_i^2} \frac{[9\tau(\kappa + \kappa_T) + \kappa]^2}{16\kappa[3\tau(\kappa + \kappa_T) - \kappa]}. \quad (A5)$$

This condition is more easily satisfied for low m mode.

For the mode which satisfies the condition $k_{\parallel} v_e \gg \omega \gg k_{\parallel} v_i$, the condition of resonant instability is easily satisfied. We have the condition for resonant instability as

$$-1 < C < 0. \quad (A6)$$

The linear growth rate is derived in the same way as the well-established local theory.

Figure Captions

- Fig. 1 Schematic configuration of current carrying plasma column. The θ -component of the magnetic field is generated by the plasma current. The longitudinal periodicity length is $2\pi R$.
- Fig. 2 Typical radial distribution. J_z is normalized to the central value and $q(r)/q(a)$ is shown. The θ -component of the magnetic field B_p is shown in an arbitrary unit. We take the radius of the plasma, a , as the current channel radius L_u , and $L_n^2 = L_T^2 = a^2/3$.
- Fig. 3 The b - η_i plane is divided into 4 regions. In the regions B and D, $\omega < 0$ holds. In the regions C and D, μ^2 is negative and the convective damping of the wave is annihilated.
- Fig. 4 Linear growth rate (normalized to ω_*) for the universal mode. We take $m_i/m_e = 1836$, $\eta_e = \eta_i = u/v_e = 0$ and $\tau = 1$. The shear parameter is indicated on each line, $\kappa L_s = 12, 20$ and 32 . Marginal stability is seen in a wide range of parameter b .
- Fig. 5 The effect of the electron temperature gradient is shown. We take $\kappa L_s = 32$, $\tau = 1$, $u = 0$. When $\eta_e > 0$, stabilization is seen. When $\eta_e < 0$, stability

is marginal.

Fig. 6 Linear growth rate of the current driven drift instability. The parameter u/v_e is denoted on each line. We take $\kappa L_s = 32$, and $\eta_e = \eta_i = 0$.

Fig. 7 Linear growth rate of the current driven drift instability in the presence of the electron temperature gradient. We take $u/v_e = .2$ and $\eta_e = 1$. The shear parameter is indicated on each line. If the shear is strong enough, the instability is suppressed.

Fig. A1 Eigen value C is shown as a function of m for the parameter $a/\rho_i = 100$.

Fig. 1

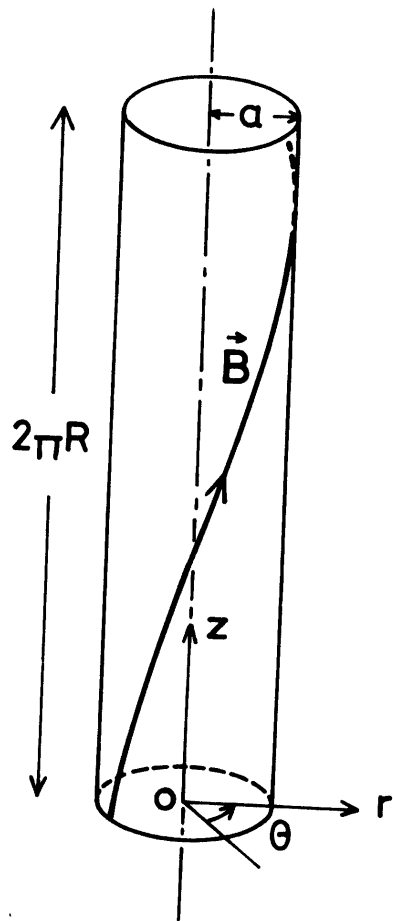


Fig. 2

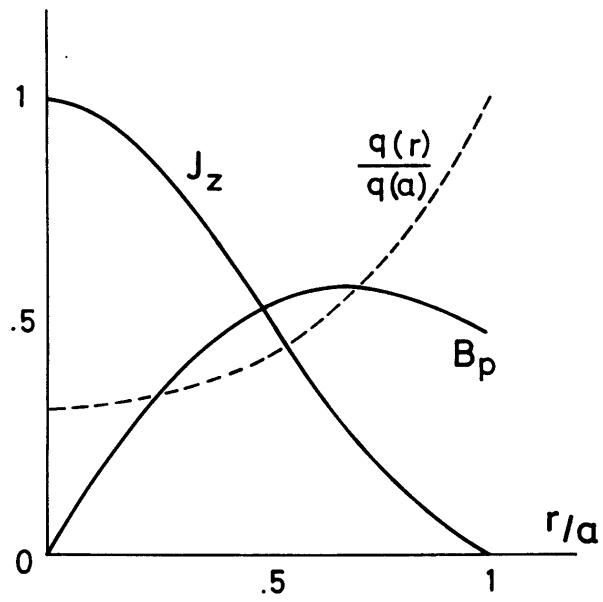


Fig. 3

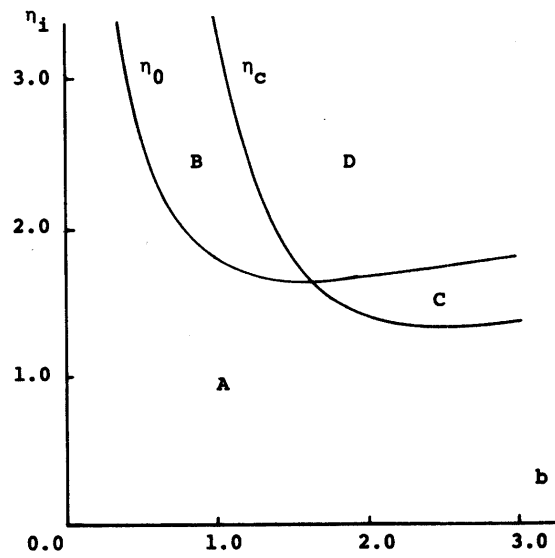


Fig. 4

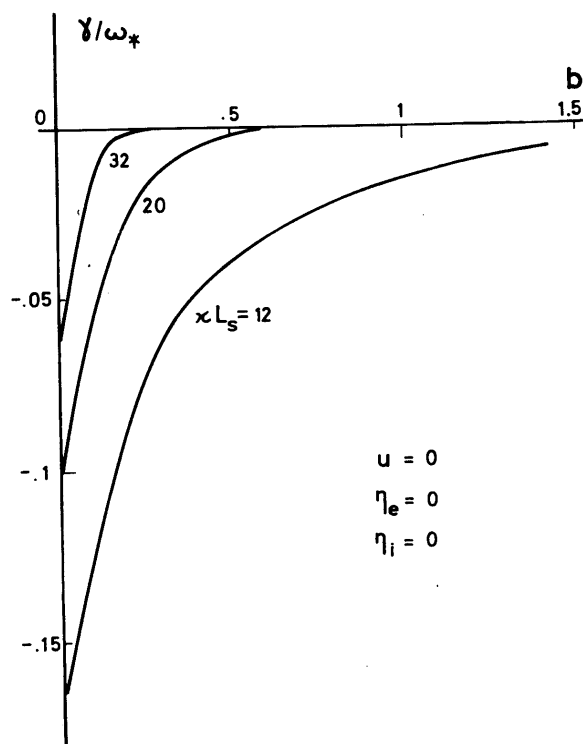


Fig. 5

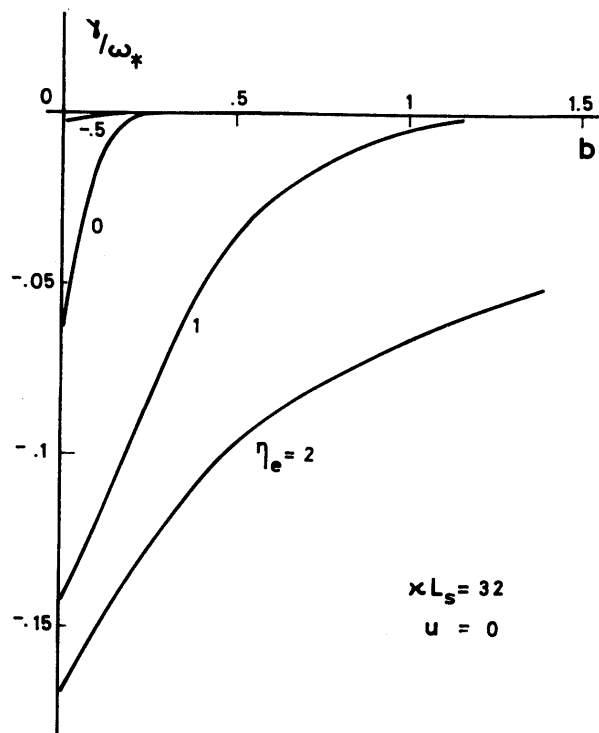


Fig. 6

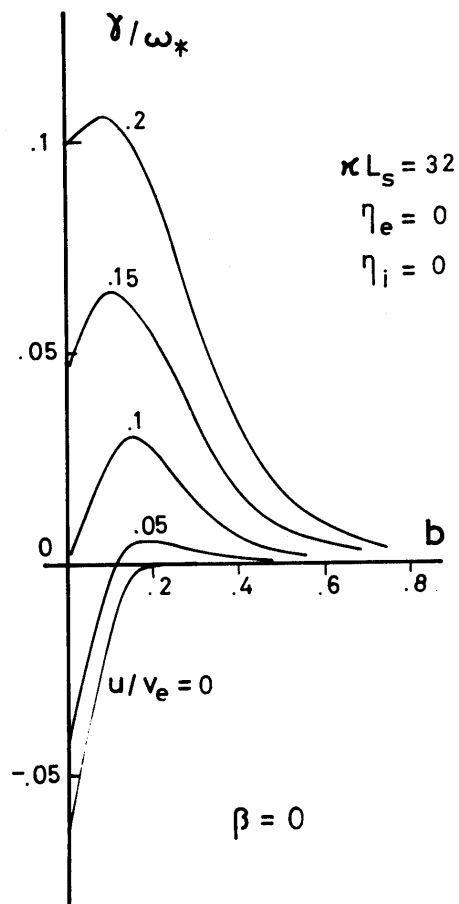


Fig. 7

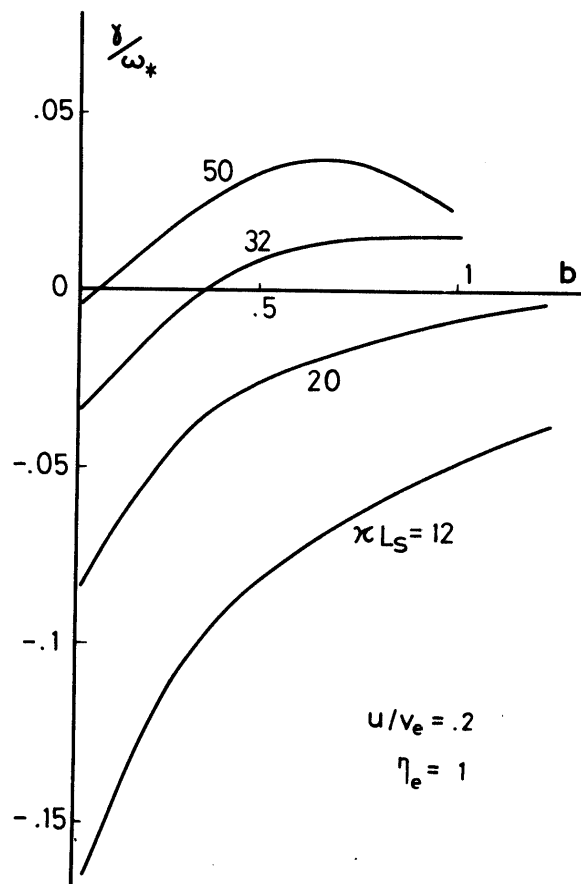


Fig. A1

